2014

Mechanical and Thermal Characterization of Continuous Fiber-Reinforced Pyrolysis-Derived Carbon-Matrix Composites

Donovan Lui
University of Central Florida

MECHANICAL AND THERMAL CHARACTERIZATION OF CONTINUOUS
FIBER-REINFORCED PYROLYSIS-DERIVED CARBON-MATRIX COMPOSITES

by

DONOVAN KAM LUI
B.S. University of Central Florida, 2011

A thesis submitted in partial fulfillment of the requirements
for the degree of Master of Science
in the Department of Mechanical and Aerospace Engineering
in the College of Engineering and Computer Science
at the University of Central Florida
Orlando, Florida

Summer Term
2014

Major Professor: Jihua Gou

ABSTRACT

Maturity of high-temperature polymer-reinforced composites defer to conventionally expensive and intensive methods in both material and manufacturing aspects. Even traditional carbon-carbon, aerogel, and ceramic approaches are highly limited by difficult manufacturing techniques and are subject to sensitive handling throughout their processing and lifetime. Despite their utility in extreme environments, the high costs of existing high-temperature composites find limited practical applicability under high-performance applications. The development of continuous fiber-reinforced pyrolysis-derived carbon-matrix composites aim to circumvent the issues surrounding the manufacturing and handling of conventional high-temperature composites.

Polymer matrix composites (PMCs) have a number of attractive properties including light weight, high stiffness-to-weight and strength-to-weight ratios, ease of installation on the field, potential lower system-level cost, high overall durability and less susceptibility to environmental deterioration than conventional materials. However, since PMCs contain the polymer matrix, their applications are limited to lower temperatures. In this study, a pyrolysis approach was used to convert the matrix material of phenolic resin into carbon-matrix to improve the mechanical and thermal properties of the composites.

Composite material consisting of basalt fiber and phenolic resin was pyrolyzed to produce basalt-carbon composites through a novel method in which the pyrolysis promoted in-situ carbon nanotube growth to form "fuzzy fibers". The carbon phenolic composites were pyrolyzed to produce carbon-carbon composites. Several types of composites are

examined and compared, including conventional phenolic and carbon-matrix composites. Through Raman spectroscopy and scanning electron microscopy, the composition of materials are verified before testing. Investigation into the improvements from in-situ carbon growth was conducted with an open-flame oxyacetylene test (ASTM-E285), to establish high-temperature thermal behavior, in addition to mechanical testing by three-point bending (ASTM-D790), to evaluate the mechanical and thermal properties of the pyrolyzed composites.

ACKNOWLEDGMENTS

My greatest appreciation goes to Dr. Jihua Gou, director of the Composite Materials and Structures Laboratory at the University of Central Florida, for advocating my graduate education and for being a wonderful advisor and colleague. Without his encouragement and sponsorship, the two years of invaluable research and experience would not be possible. I am ever grateful for the opportunities that working with you has garnered.

Thank you to my thesis committee, Dr. Seetha Raghavan and Dr. Kuo-Chi Lin, for taking time to endorse the culmination of my graduate experience and for the endless insight and assistance they have provided to my research and education.

To my esteemed friend and brother, Ricky McKee, the utmost thanks and credit for the endless hours spent working together on this research among many other projects. Your friendship and support is undeniably vital to this achievement.

Most of all, I want to recognize my family for the unending support and love that has brought me so far in life. I am forever thankful for everything you have given me. Your sacrifices have inspired me to pursue the greatest opportunities and to push myself as far as I can imagine. Mom and Dad, this thesis is for you, as a commemoration of all you have endured for Ashley and myself, and for the opportunities you have given us.

I would also like to thank:

Gregory Freihofer and Albert Manero for assisting with Raman spectroscopy.

Erik Durnberg for assisting with three-point bending tests..

Xin Wang assisting with scanning electron microscope imaging.

John Sparkman for selflessly endangering your hand in the name of science.

Tim Lindner for irreplaceable assistance in machining and manufacturing.

David Reel for making the majority of the tooling for processing and testing.

Fei Liang for sharing your knowledge of composite processing.

Jason Gibson for sensible wisdom and advice in composite manufacturing.

TABLE OF CONTENTS

LIST OF FIGURES

LIST OF TABLES

LIST OF ABBREVIATIONS

CVD   Chemical Vapor Deposition

EDX   Energy-Dispersive X-ray Spectroscopy

FRC   Fiber-Reinforced Composite

HTC   High-Temperature Composite

PMC   Polymer Matrix Composite

PPR   Pyrolyzed Phenolic Resin

RS   Raman Spectroscopy

SEM   Scanning Electron Microscopy

TGA   Thermogravimetric Analysis

CHAPTER ONE: INTRODUCTION

Fiber-reinforced composites (FRCs) have come to the forefront of alternative material solutions to create lighter, cheaper, and even more effective substitutes for traditional uses. Composite materials demonstrate high stiffness, high specific strength, and excellent fatigue properties among other positive durability characteristics that benefit their use for a multitude of purposes. [1] In terms of mechanical and thermal loading, polymer-matrix composites (PMCs) represent a popular option, however the nature of these FRCs include positive and negative material characteristics. The aim of this research is to utilize desirable properties, such as good erosion and chemical resistance, while eliminating disadvantageous properties, such as matrix voids/defects and planar/interlaminar anisotropy.

1.1   Motivation

There exist a spectrum of drawbacks that accompany the benefits of designing, processing, and utilizing composite materials in mechanical and thermal applications. Optimizing specific properties of composite materials for extreme environments can be both challenging and expensive, leading to restrictive use and sensitive selection and handling of such materials. The most difficult area of composite tailoring arises in the field of mechanically viable, yet thermally stable, high-temperature composites (HTCs). In the various conditions that composites experience, the material will undergo both physical and chemical changes induced by thermal, velocity and pressure loadings, leading to mass loss and surface recession. [1, 5] These loadings lead to several distinct failure mechanisms that provide massive drawbacks to the application and design of composite materials. Primarily

1

the degradation of material in extreme environments and conditions reduce the integrity of both fiber reinforcement and the matrix alike, leading to mechanical failure by delamination, loss of strength, and erosion.

Careful consideration is necessary to implement a cost-effective and useable design of HTCs. Research performed on basalt fibers and phenolic resins present an appealing option to solve the issues surrounding high-temperature applications. Basalt fiber is a competitive fiber to glass and carbon fibers. While exhibiting good chemical resistance and strength-to-weight ratio, basalt is also highly abundant and free of health and environmental hazards. Combined with the multitude of thermal applications, basalt fiber is an excellent alternative to explore greater economy. [7, 9, 10] Phenolic resin demonstrates low flammability, degradation resistance, low thermal conductivity, and high specific strength. [26] Resole-type phenolic resins have long been used for thermomechanical applications such as insulation and fire-resistance. [34] Despite the evidence of both materials being applicable for high-temperature purposes, very little research exists on the properties of fiber-reinforced basalt-phenolic composites. Additionally, phenolic resin is an excellent binder for carbon composites, as it transforms into pyrolytic carbon at elevated temperatures. [29] An in-depth exploration into the properties of basalt-phenolic composites is prudent, along with its converted pyrolytic carbon-matrix counterpart.

1.2   Research Methods

1.2.1   Design of High-Temperature Composites

When designing HTCs, several factors are of primary concern. Experimental data shows that it is more prudent to lower surface-normal thermal conductivity than increase mechanical strength. [3] However mechanical integrity should always be considered as the survivability of the composite material is crucial to effectiveness in high-temperature environments. To address surface-normal thermal conductivity, two approaches represent viable solutions; one is to increase the through-thickness anisotropy, the other is to increase the in-plane conductivity. An increase in through-thickness anisotropy has a direct correlation to the delamination of the composite as mismatches in properties lower the effective lifetime of the material significantly. This leaves increasing the in-plane thermal conductivity as the most sensible solution.

1.2.2   High-Temperature Composite Fabrication

HTCs display an array of material characteristics, but all such substances demonstrate an innate ability to dissipate heat while maintaining mechanical integrity. Convective heat flux is balanced within the composite material via conduction, surface radiation, and chemical reactions/phase transitions. [1] These mechanisms complicate the design of HTCs as the evolution of these phenomena severely alter the material structure. The difficulties in managing complex heat transfer and phase progressions suggests that a mechanical approach poses a feasible solution to survivability of thermomechanical events. By controlling mechanical aspects of the composite through fabrication, integrity will be ensured in a consistent fashion towards the development of useable and cost-effective

material. In a concise approach, high-temperature performance is directly correlated to density and void content of the composite material. [5] This focus is a highly controllable method through careful selection of materials and processing techniques. Through in-autoclave processing and low-temperature treatment practices, a basalt-carbon composite will be explored and compared to existing high-temperature materials.

1.2.3   Objectives

This research aims to use pyrolysis to induce an in-situ growth of carbon throughout the composite laminate by converting the polymer matrix into carbon. A novel approach using basalt fiber and phenolic resin has shown that pyrolysis instigates annular growth of carbon on the continuous basalt fiber reinforcement. Extending this approach into continuous FRC laminates several outcomes are anticipated, all of which are predicted to alter the mechanical and thermal characteristics of continuous FRCs.

The overall aim is to improve the effective density of FRC structures by reducing the porosity of composite matrix. The mechanism of pyrolysis is used to convert the polymer matrix into a carbonaceous residue that modifies both mechanical and thermal characteristics under applied loadings. Losing the polymer matrix during pyrolysis changes the mechanisms that govern the behavior of FRCs significantly, and these changes will be mechanically and thermally evaluated. It is anticipated that the growth phenomenon will mitigate the delamination of fiber plies under thermal loading by creating a better interface between fiber and matrix to improve both thermal and mechanical properties.

1.3   Structure of the Thesis

The structure of this thesis will follow the manufacturing, processing, testing, and evaluation of the continuous basalt-fiber-reinforced carbon-matrix laminate. Corresponding phenolic and carbon-matrix counterparts encompassing more traditional approaches to HTCs will also be explored in a comparative effort and to establish working baselines. Methodology and theory will be discussed in congruence with experimental results, with a summation of experimental findings afterword.

Firstly, principles of carbon development in pyrolysis will discussed in-depth along with its relation to carbon-matrix composites. Theory and practice is explained relating to the decomposition of phenolic resins and hydrocarbons in general. This knowledge is applied to the mechanism of pyrolytic carbon growth by means of chemical vapor deposition (CVD), which is a standard and commonplace process to initiate carbon development. This type of carbon has particular relation to thermal and mechanical properties when applied to FRCs and also to high-temperature mechanisms as well.

Secondly, the selection and design of composite materials will be addressed. The means of manufacturing the continuous FRCs and the pyrolysis treatment is discoursed to glean a better understanding of the processing and to draw a picture of the intended effects this research intends to observe. Also detailed are the testing environments to which all of the samples will be subjected to in order to define a useful parameterization of the baseline characteristics and to measure changes in properties from the pyrolysis treatment.

Thirdly, a confirmation of the novel basalt-carbon material will be detailed in full to verify the evolution of the mechanisms stated from theory and practice. Several material characterization techniques are used to distinguish the morphology of the derived novel material. The resulting experimental data will be presented to garner the data in order to define the thermal and mechanical effects of the pyrolysis treatment. Pertinent material properties will be calculated as detailed in the applied ASTM test standards.

Lastly, a discussion of the findings and applicable future work will be explored, A final assessment of the new basalt-carbon material will be made along with suggestions for continued investigations into the technique and optimization of the process.

CHAPTER TWO: LITERATURE REVIEW

2.1   Development of Carbon in Pyrolysis

CVD is the common method used for infiltrating pyrolytic carbon onto substrates and FRCs. [11] In converting polymeric matrices into carbon, several factor must be considered. The pyrolysis mechanism necessitates specific tailoring to the decomposition of hydrocarbons within the polymer matrix as well as the thermal characteristics of the reinforcing fiber. A vast amount of research into this topic suggests that mass growth rate is independent of reaction temperature between 700 and 850°C. [12] Furthermore, it is well established that CVD of carbon at low temperatures between 800-1200°C is a main method for manufacturing carbon/carbon. This method leads to excellent interface bonding, low residual stress, and little damage to the fiber. [28] As an extension, this concept is applied towards the enhancement of continuous basalt FRCs, as the annular carbon interphase of the basalt fibers influences properties in the fiber-dominated direction, improving reinforcement and interfacial properties. [7, 8]

2.1.1   Decomposition of Phenolic Resin

Experimental data shows that carbonaceous residue (i.e. char) is a well-established means to augment the fire retardancy of composites. [1] In this research, phenolic resin is used to form carbon from condensation reactions of polycyclic aromatic hydrocarbons. [19] The decomposition of phenolic resin is generally represented by three stages, beginning at 300°C. Experiments show that a large reduction of resin weight in the composite occurs in the two early stages from additional formation and breaking of crosslinks, before the eventual breaking of cyclic hydrocarbon bonds to for pyrolytic

carbon in the latter stage above 600°C. [31, 32] A substantial downside to using polymer matrix precursors for carbon development is the need for densification by CVD to achieve desired the density and mechanical properties. [30] Fortunately numerous investigations confirm phenolic-matrix composites effectively form char during heating. [4, 5, 6]

Phenolic resin undergoes a significant amount of weight loss as well as volumetric shrinkage under pyrolysis. This pyrolyzed phenolic resin (PPR) product is distinctly black, hard, and glassy, unlike its opaque polymeric phenolic predecessor [Figure 1]. When pure phenolic is pyrolyzed, a noticeably dense carbon-matrix is left behind, as shown by scanning electron microscopy (SEM) imaging [Figure 2]. The flakes and buds shown in Figure 2 are indicative of amorphous carbon, am expected product of pyrolysis. A tight packing of carbon residue is anticipated in a similar manner when processing FRCs with a high resin content, likely following similar weight loss and areal shrinkage.

Figure 1: Pure phenolic resin and PPR
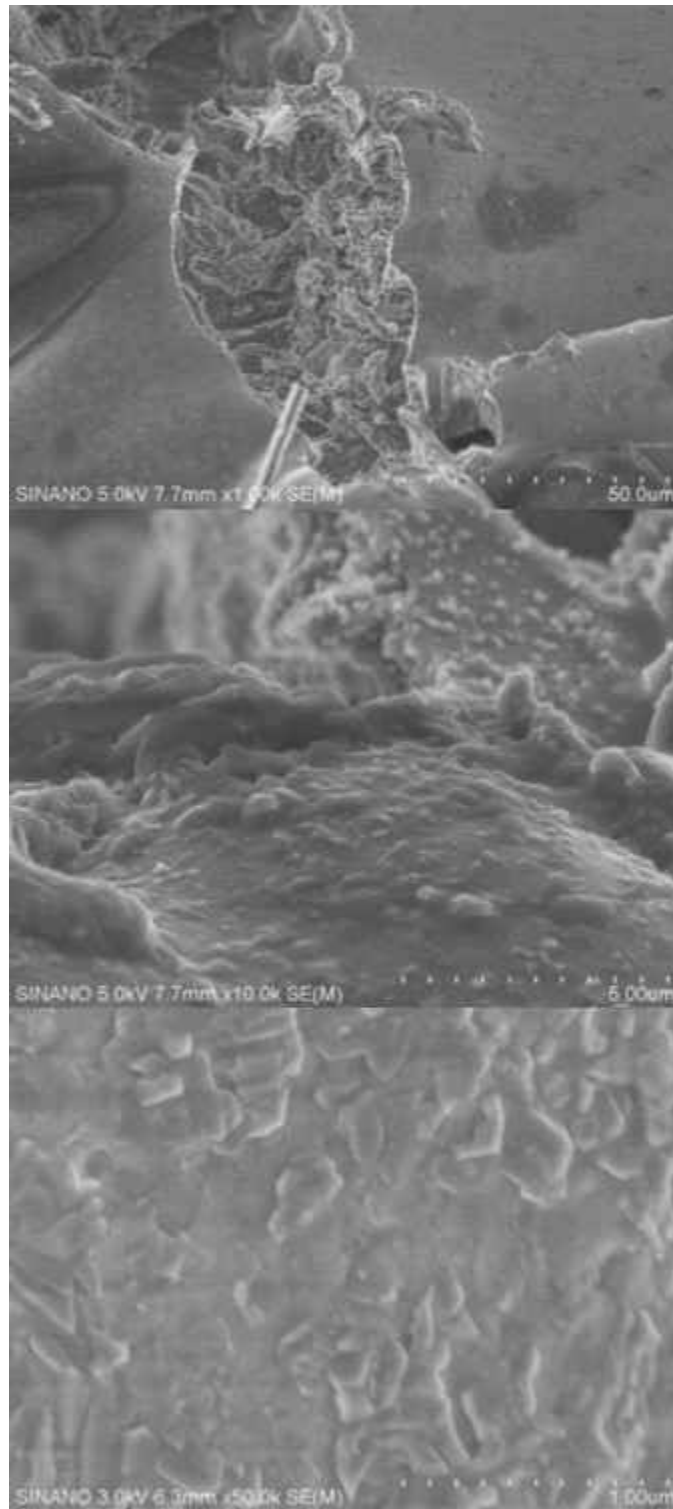
Figure 2: SEM images of pure PPR

2.2 Carbon-Matrix Composites

Carbon-matrix composites with continuous fiber reinforcement is used as a conventional material for high temperature applications. Carbon-carbon composites are a commonplace example used in a host of applications. Most notably, carbon-carbon composites find use as thermal protection material for ablative purposes. Large amounts of data verify that carbon-matrix composites maintain strength and modulus at high temperatures. [30] The production of carbon-matrix composites are done in a multitude of methods, most with notably CVD and pyrolysis.

2.2.1 Mechanical Properties

Thermal mismatches between the matrix and fiber cause an open interface of the fiber and matrix which reduces the effectiveness of the composite under loading. [5] This is particularly the case with polymer-matrix composites as large dissimilarities in materials properties can exist between fiber and matrix. Even with phenolic-matrix composites, the low thermal conductivity of phenolic resin can force a mismatch with fiber reinforcement, leading to failure. Additionally, varying coefficients of thermal expansion produce residual thermal stresses within the composite during processing. Homogenizing the composite properties across the leads to evenly distributed compressive residual stresses that increase the mechanical strength and mitigates delamination and cracking. [27]

It is proven that the addition of micro/nanocarbon can enhance interfacial bonding. High interfacial strength reduces the possibility of mechanical failure. [3, 7] Furthermore, carbonization of phenolic changes failure to matrix-dominated brittle fracture, rather than the fiber dominated pull-out failure normally exhibited by polymer-matrix composites.

[30] The conversion of the polymeric matrix into carbon aims to take advantage of the mechanical improvements from the homogenization and densification of the material.

2.2.2   Thermal Properties

Thermal properties have a drastic effect on mechanical integrity. Weight is lost during extreme temperature exposure mainly from surface erosion and not thermal decomposition. [2] Fundamentally, a survivable material structure is crucial to the effectiveness of HTCs. Survivability can be improved through managing the temperature gradient by controlling both the in-plane and through-thickness thermal characteristics of the composite. Carbon-matrix composites exhibit better equated thermal properties between the fiber and matrix which suggest that a synergistic complete composite mechanism is a worthwhile venture in improving overall thermal performance.

Primarily the reduction of temperature gradient in the through-thickness laminate direction induces a more uniform expansion/contraction which increases mechanical integrity. Furthermore, homogenized properties relieve thermal stress upon flame exposure and decrease thermal stresses experienced from continued heating. [26] Experiments have shown that the existence of carbon reduces the surface-normal heat transfer in the composite. [2] This is due to the ordered carbon within composites providing conductive pathways and mechanical bridging, inducing a reduced property contrast within the composite material. [25]

CHAPTER THREE: METHODOLOGY

3.1   Fiber-Reinforced Composite Preparation

Autoclave processing has long been used as an effective method to manufacture composite materials with consistent parameters. All of the FRC laminates used in this research are processed in the same fashion. A unique in-autoclave cycle and bagging technique was developed to ensure the highest possible resin content ($\approx$40% by volume). High resin content was desirable to maintain consistency between all samples, and for the purpose of resin-to-carbon conversion under pyrolysis. The panels consist of a layup of $[0/90°]_n$ plies; the number of plies is carefully calculated in conjunction with the desired resin content and for sample size requirements outlined for the testing standards. Four types of FRC laminates are manufactured and tested for this research: carbon-phenolic, carbon-carbon, basalt-phenolic, and basalt-carbon. Each type of laminate was consistently manufactured according to the reinforcing fiber; the same fiber ply orientation, number of plies, total processed thickness, and initial polymeric content.

Figure 3 shows an unpyrolyzed basalt-phenolic laminate sample used for initial characterization. The macroscopic geometry of the fiber is well-retained as evidenced by the grid-like appearance and edge fraying. Qualitatively, the laminate is extremely rigid, as expected from the established understanding of the mechanical properties of the fiber and matrix. It is of note that no issues presented themselves in cutting the sample; no delamination, cracking, evidence of voids, or fiber pull-out occurred.

Figure 3: Unpyrolyzed basalt-phenolic laminate

<u>3.2   Fiber-Reinforced Composite Pyrolysis</u>

Pyrolysis removes thermally unstable components from the polymer matrix while potentially improving physical properties. Combined with the residual thermal stressing of the fibers from pyrolysis can affect the mechanical characteristics greatly. [8] Polymeric materials experience thermal shock from thermal stressing (expansion and contraction of components). [26] The conversion of the matrix into carbon relieves the thermal shock under loading, as well as evenly applying a compressive prestressing of the fibers during processing. While the matrix is readily converted into a desirable product, the structure of the fibers must be considered. Primary weight loss at lower temperatures is due to degradation of the phenolic-matrix, while higher temperatures induce physical and chemical changes in the fiber. Stimulating pyrocarbon growth can increase the density of the composite and improve the interface between fiber and matrix. This decreases the inequality of thermal coefficients as well as minimizing the material mass loss of fiber and matrix during thermal loading. [5] However, even a minute change in the fiber properties,

13

integrity, or geometry can significantly affect the synergistic behavior this pyrolysis process is attempting to attain.

When focusing on the specific design of the proposed basalt-carbon material, the decomposition of phenolic into carbon is used in conjunction with the concepts of pyrocarbon infiltration for carbon-matrix composites. As previously stated, CVD is a proven method to induce carbon growth on substrates. However, when a substrate is not conducive to carbon growth, a catalyst agent is compulsory. Research has shown that iron is one of the most effective metal catalysts for carbon growth. [17, 18] Furthermore, iron catalyzed carbon growth has been highly characterized and optimized between 650-800°C. [14] In terms of basalt-carbon, this temperature range has a meaningful correlation to the working temperature of the fiber. Beyond 700°C, basalt fiber begins to soften, which causes iron particles within the basalt fiber to migrate to the surface of the fiber. This surfacing phenomena acts as a catalytic growth site for the development of carbon, while only slightly damaging the structure of the fiber.

Figure 4 shows a pyrolyzed basalt-phenolic laminate sample used for initial characterization. The macroscopic geometry of the fiber is well-retained as evidenced by the grid-like appearance and edge fraying. Qualitatively, the laminate is rather rigid, however not so much as it's basalt-phenolic counterpart. Also, the sample exhibits a visible glassy texture, as expected from the conversion of the matrix. It is of note that no issues presented themselves in cutting the sample; no delamination, cracking, evidence of voids, or fiber pull-out occurred.

Figure 4: Pyrolyzed basalt-carbon laminate

The pyrolysis of the FRC laminates is performed in a specially design kiln, made for the injection of inert atmosphere under minimal pressure and flow rate, with additional hydrocarbon addition to stimulate additional carbon growth within the FRC laminate. A uniquely derived process tailored specifically for the basalt-carbon material composition is used for pyrolysis to ensure the retention of fiber properties and geometry with regards to the integrity of the material. This process is based in the principles of CVD carbon growth processing in concurrence with particular considerations of basalt fiber reactions.

3.3   Thermal Testing

3.3.1   Open-Flame Oxyacetylene Testing

Thermal characterization is performed using an oxyacetylene torch in correspondence with the guidelines set forth in ASTM-E285. Using a neutral flame burned at a 1:1 stoichiometric ratio, the laminates are impinged upon from a surface-normal

direction. At 25.4mm from the torch tip, where the test sample is placed, the measured heat flux is 535 W/cm^2. This testing also introduces a velocity and pressure impingement along with the thermal loading. The sample area is 101.5x101.5mm, and the thickness is 6.35mm, as required by the standard. Front-face impingement is performed at the center of the panel. Back-face temperature measurements are taken using a thermocouple placed at the center in line with the torch tip. Figure 5Figure 7 shows a still frame of the ASTM-E285 testing.
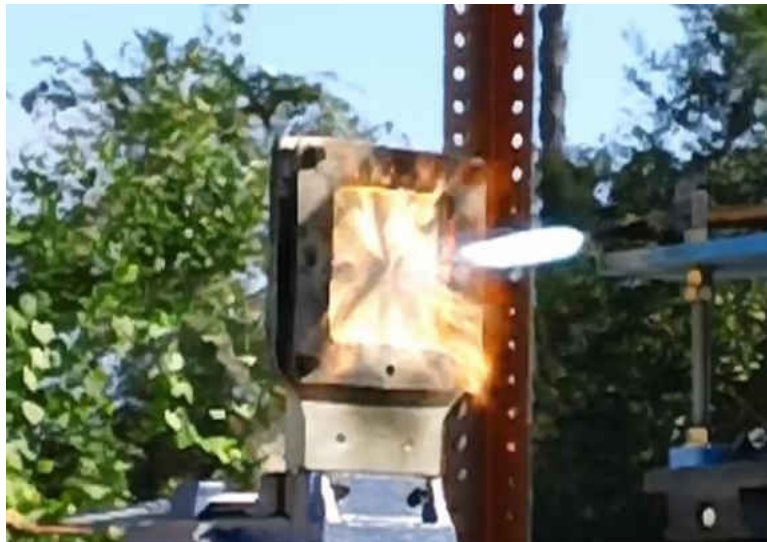

Figure 5: ASTM-E285

Time and temperature from initial flame impingement until burn-through is measured. Several calculations are made from the gathered data, measuring the insulation and erosion rate of the material. From these fundamental experimental values, the materials are indexed and compared on a unified basis to determine thermal effectiveness.

3.4 Mechanical Testing

3.4.1 Three-Point Bending

Three-point bending is a commonly used method to initially characterize the mechanical effectiveness of FRC laminates. Failure of composite laminates stems from delamination that propagates from first ply failure. This test applies maximum stress at the outer ply of the laminate at a predetermined continuous strain rate. ASTM-D790 defines a constant strain rate of 0.01 mm/mm/min as standard procedure. For high-strength reinforced composites, a span to depth ratio of 60:1 is used to eliminate shear effects when establishing modulus. It is of note that the calculated modulus is a product of the ply stacking sequence, which is not necessarily indicative of the tensile modulus of the material.

Figure 6 shows the actual three-point bending test fixture and sample. The samples are preloaded to 1N and bent at a crosshead speed of approximately 1 mm/s. A span of 127mm is employed to ensure pure bending and no shear stresses, and in an attempt to induce a large bending stress in hopes of observing plasticity or even failure. Time, strain, displacement, and crosshead speed are measured to establish modulus value for the FRC laminate samples. From these values several important parameters are calculated.

Figure 6: ASTM-D790

CHAPTER FOUR: FINDINGS

4.1   Pyrolysis Morphology of Basalt-Carbon

Experiments show that phenolic almost disappears at 600°C. There is a rapid weight loss up to this temperature from the decomposition of phenolic. [30] Initial investigation into this occurrence was performed at a small scale, using a thin laminate in a tube furnace. Two types of samples were tested in the tube furnace using the pyrolysis cycle derived for this research: a basalt-phenolic sample without additional hydrocarbon added, and a basalt-phenolic sample with additional hydrocarbons added.

Figure 7 shows pyrolysis sample without hydrocarbon addition. As shown by the SEM image, the bare fiber retains the general fiber geometry with miniscule amounts of deformation. The lack of distortion suggests that designed cycle is suitable for basalt fiber.
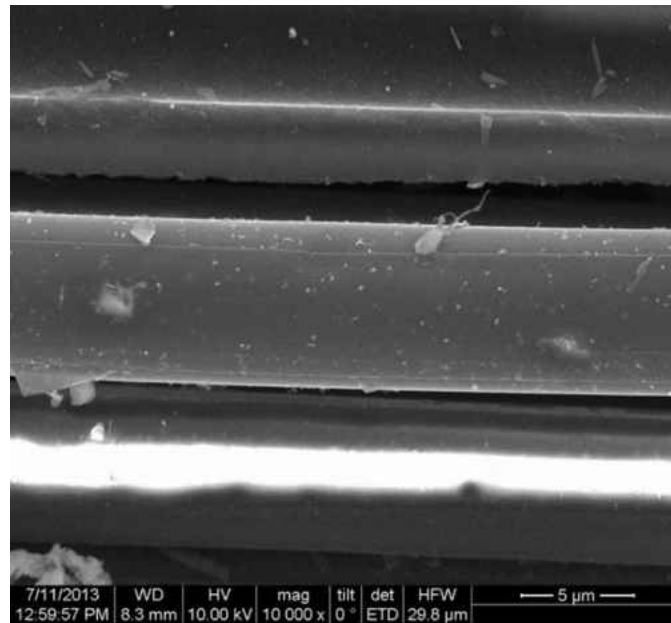

Figure 7: SEM image of bare basalt fiber

Figure 8 shows pyrolysis sample with hydrocarbon addition. As shown by the SEM image, a large amount of fibrous growth is deposited on the basalt fiber. The development of the ordered carbonaceous residue suggests that designed pyrolysis cycle is suitable for the growth of pyrolytic carbon on basalt fiber. It also demonstrates the existence of iron in the fiber and the migration of the iron particles at temperature from the softening of the basalt fiber, as predicted. Note that carbon deposition is governed by heterogeneous surface reactions that favor low pressures and increasing surface area-to-volume ratios. [15, 23] This was demonstrated at a small scale from this experiment as evidenced by the clear structure of the pyrolytic carbon development in tube furnace conditions.

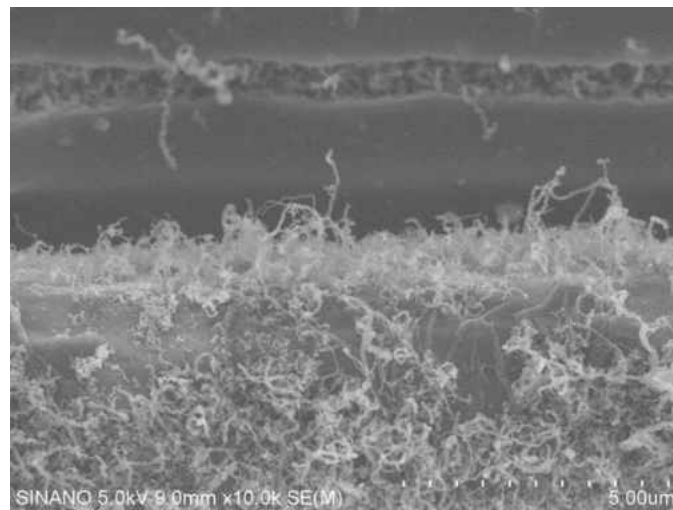Figure 8: SEM image of basalt fiber with carbon growth

The carbon growth on the basalt fiber is highly reminiscent of "fuzzy fibers". Fuzzy fibers have long been explored as an effective means to improve composite properties, both thermally and mechanically. Experiments show that fuzzy fibers strengthen the interface between the fiber and matrix by improving interface strength and bridging. Additionally,

this type of fiber possesses multifunctional properties as well as improved transverse properties. [24] Traditionally, the "fuzz" is grown on the pure fiber substrate, usually by CVD or printing, then either prepregged or included in a wet layup. This procedure is tedious and adds complexity and cost to production. An in-situ growth of "fuzz" potentially removes the extra stages in production, and possibly eliminates chemical waste.

With the confirmed development of carbon growth on basalt-fiber from the designed pyrolysis cycle, scaling of the laminate is performed to manufacture proper sized laminate panels for ASTM-E285 testing. Three different non-destructive characterization methods are employed to confirm the existence of carbon within the pyrolyzed composite structure. Additionally, the thermal stability of the material is evaluated on a small scale.

4.1.1   Scanning Electron Microscopy

SEM imaging is used as a visual technique to verify the development of carbon residue from the decomposition of phenolic resin and the growth from the basalt fiber. The existence of carbon is conducive to SEM imaging, as the conductivity of both the carbon and basalt fiber do not require the sample to be pretreated for analysis. Figure 9 clearly shows a carbonaceous residue developed on the fibers. It can be seen that the carbon adheres to the fiber proximity with a distinct lack of carbon in the areas between fibers. This is indicative of a complete removal of the phenolic-matrix, either by conversion into carbon or by evolution into gases carried away by the flow of injected inert gas.
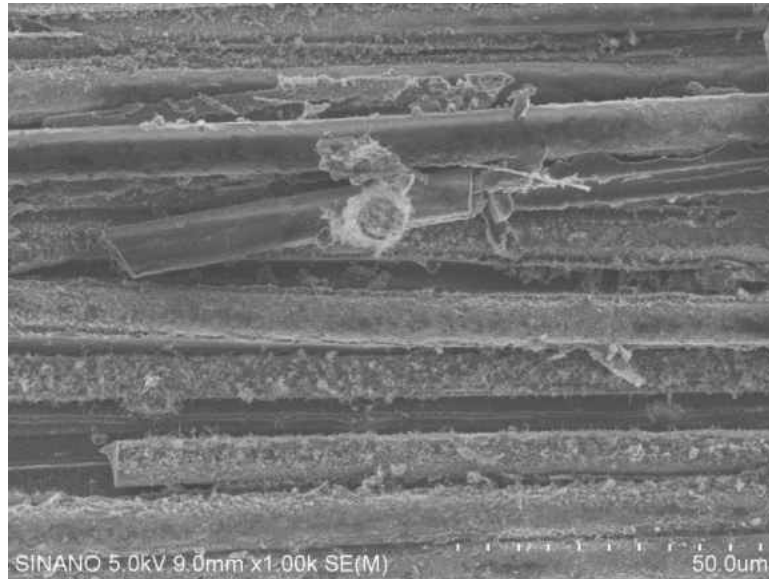
Figure 9: SEM image of basalt-carbon composite

From Figure 9, several key visuals can be delineated. Most significantly, a clear identification of residue is adhered to the fiber surface in an annular fashion. While a highly distinctive "fuzzy" characteristic is partially lacking, the image still shows that a conversion of the phenolic-matrix has occurred coinciding with a carbon growth situated on the fiber surface. The budding nature of the carbon residue is likely a result of reactions away from catalytic sites, which are shown to lead to amorphous carbon. [17, 18]

Figure 10 demonstrates the carbon growth on a more macroscopic scale. When viewing the pyrolytic matrix from this aspect, the most noticeable feature is the fiber-matrix density of the composite. One of the objectives of this research was to densify the composite material; pyrolysis of the basalt-phenolic achieves that. Also noticeable is the large amount of amorphous carbon accompanying the fiber growth. This achieves the goal of reducing the porosity of the material via tighter packing of fiber and matrix.

22

Figure 10: SEM image of basalt-carbon composite

4.1.2　Energy-Dispersive X-ray Spectroscopy

Energy dispersive X-ray spectroscopy (EDX) is a powerful accompaniment to SEM for additional non-destructive characterization. This tool sho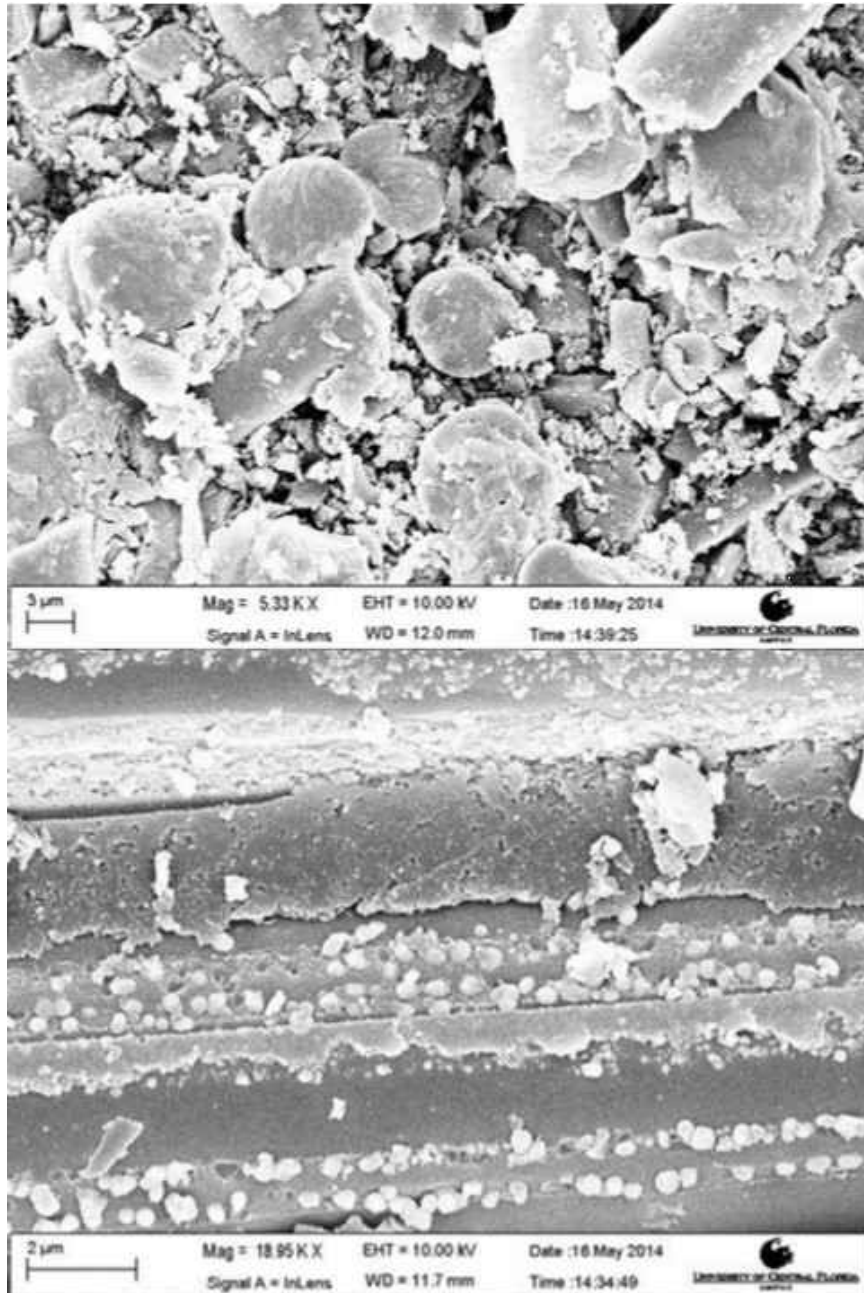ws the atomic breakdown of the material composition by stimulating the unique emission characteristics of each element. The excitation of the electrons in specific orbital shells emits X-rays that register at different intensities. These intensities are what distinctively identifies the elements. Figure 11 presents a table of weight content of a grown carbon "bud" located on the basalt-fiber from pyrolysis. The individual letter index next to the element abbreviation indicates which electron shell was excited; "K" is also known as the 1-shell and "L" is commonly known as the 2-shell. Iron (Fe) vibrates in the 2-shell because it is a transition metal, unlike the other elements that register in the 1-shell (the closest shell to the nucleus). The existence of iron immediately implies the growth of the carbon on the fiber, as discussed previously. The other elements are also significant, obliging a necessary discussion of the EDX results.

Basalt fiber is a naturally iron/iron oxide (Fe, FeO) rich material that also contains high amounts of tectosilicates. Tectosilicates encompasses a broad spectrum of quartz/silica (SiO_2) based materials. The majority of these tectosilicates also incorporate aluminum (Al) into their structure as well. All of these elements are abundant and register with significance in the EDX shown in Figure 11. However, carbon (C) is the most abundant of all, suggesting that the "bud" is a solid constituent of the pyrolytic deposition and the trace values of the other elements are representative of the fiber substrate.
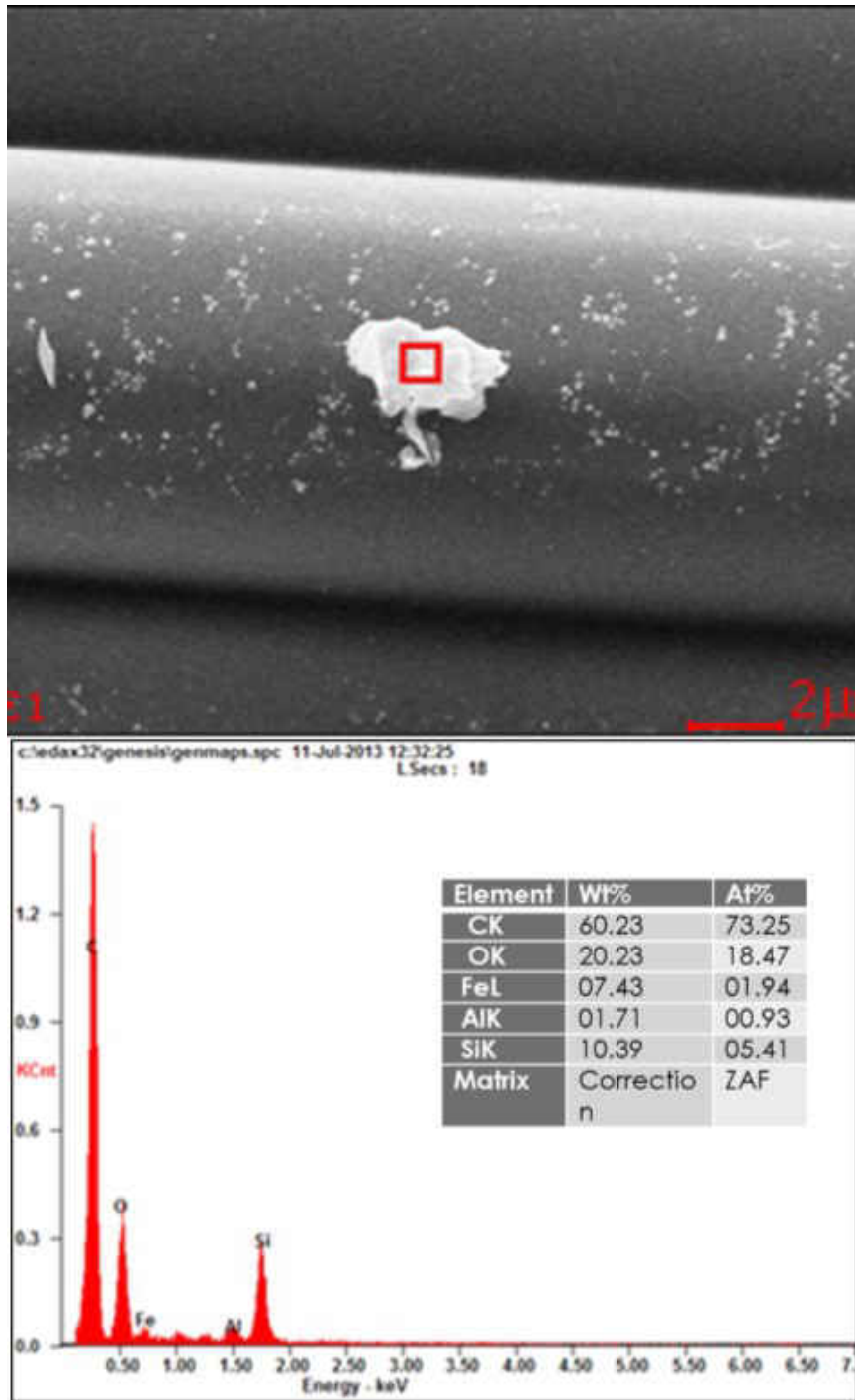
Element	Wt%	At%
CK	60.23	73.25
OK	20.23	18.47
FeL	07.43	01.94
AlK	01.71	00.93
SiK	10.39	05.41
Matrix	Correction	ZAF

Figure 11: EDX of carbon growth on basalt fiber

4.1.3 Raman Spectroscopy

Raman spectroscopy (RS) is an exceedingly useful tool for non-destructive characterization. All carbon allotropes are active in RS. Specifically, the position, width and intensity of the measured vibrational bands unmistakably determine the order of the carbon structure. [20] Four particular RS peaks epitomize carbon structures. Radial breathing mode around 100-300 cm^{-1} indicate SWNT D and G bands between 1350-1590 cm^{-1} determine purity. The existence of a G' band, usually above 2000 cm^{-1} indicates a graphitic structure related to carbon whiskers. The G' band has an effect on the intensity of the D and G bands due to it registering only for unique carbon structures between graphite and carbon nanotubes. [13, 20, 21, 22, 23]

Figure 12 shows the RS plot for the basalt-carbon laminate used for ASTM-E285 testing. The most noticeable peaks are the D and G peaks. A wide D peak designates a large amount of amorphous carbon, likely associated with the pyrolytic decomposition of the phenolic-matrix. This is further suggested by the peak intensity ratio of the D and G peaks, signifying a low purity of highly organized carbon (i.e. nanotubes). Despite the I_D/I_G ratio, there is a slight RBM peak, which would intimate a small growth of carbon nanotubes. It is likely that the small ordered carbon growth is a consequence of the hydrocarbon precursor size and a function of the precursor's ability to fully and effectively penetrate the laminate through the entire thickness. Additionally, the presence of other carbon forms reduce RBM and D band intensity. [16] Nevertheless, RS shows that a degree of pyrolytic carbon is achieved in the pyrolyzed basalt FRC.
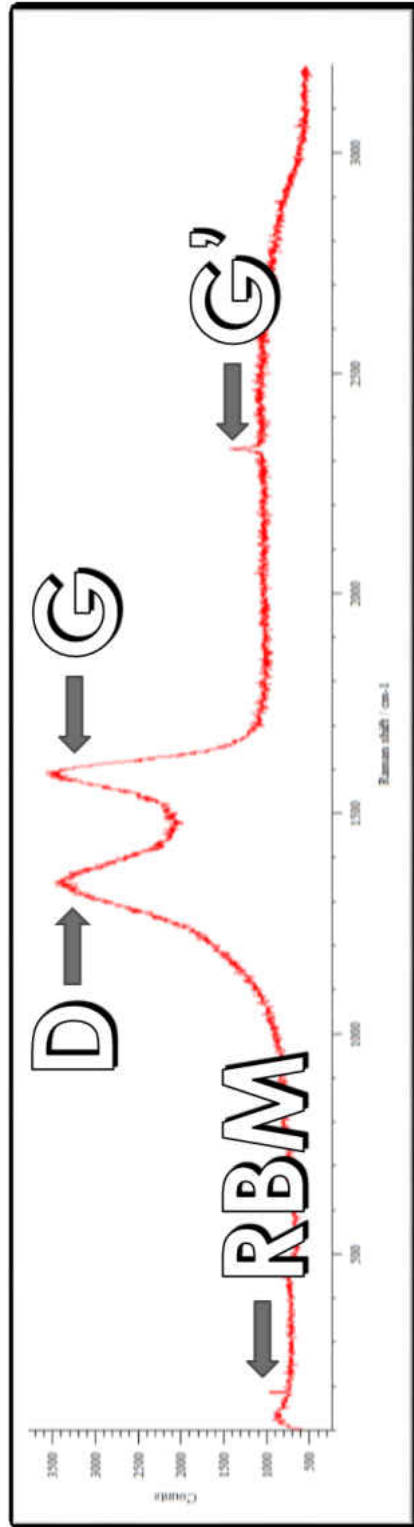
Figure 12: RS of basalt-carbon composite

27

4.1.4 Thermogravimetric Analysis

Thermogravimetric analysis (TGA) is the only destructive method used to initially characterize the basalt-carbon composite, and the only thermal test method used as a forerunner to the oxyacetylene testing. The mass loss was measured over increasing time and temperature, as presented in Figure 13. In inert atmosphere, the pyrolyzed basalt-carbon sample was heated to well over 1100°C. It is clear that no significant physical or chemical changes: water evolution, and mass addition or subtraction occurred. Additionally, no mechanical failure manifested during TGA, posing interesting questions in regards to the applicability of this material.

Remarkably, the thermal mass stability of the basalt-carbon at high temperatures is more symptomatic of carbon than of basalt. With no secondary phase transitions or combustion, and very low decomposition evident from the TGA testing, the indication is that the basalt-carbon material has drastically diverged from its fibrous properties. Most notably the material retains well over 99% of its mass up to 700°C with only a miniscule mass loss rate. This occurrence is a vital phenomenon that details important details about the material composition. Well represented in Figure 13, the mass loss rate stays nearly linear until the 600°C threshold. At this temperature, the percentage of mass loss also diverges from its initial slope. Both trends show that this material is highly stable until the softening of the basalt fiber begins to occur. Additionally, this verifies that the designed pyrolysis cycle retains the majority of basalt fiber properties as intended, and also satisfies some of the objectives set for this research.
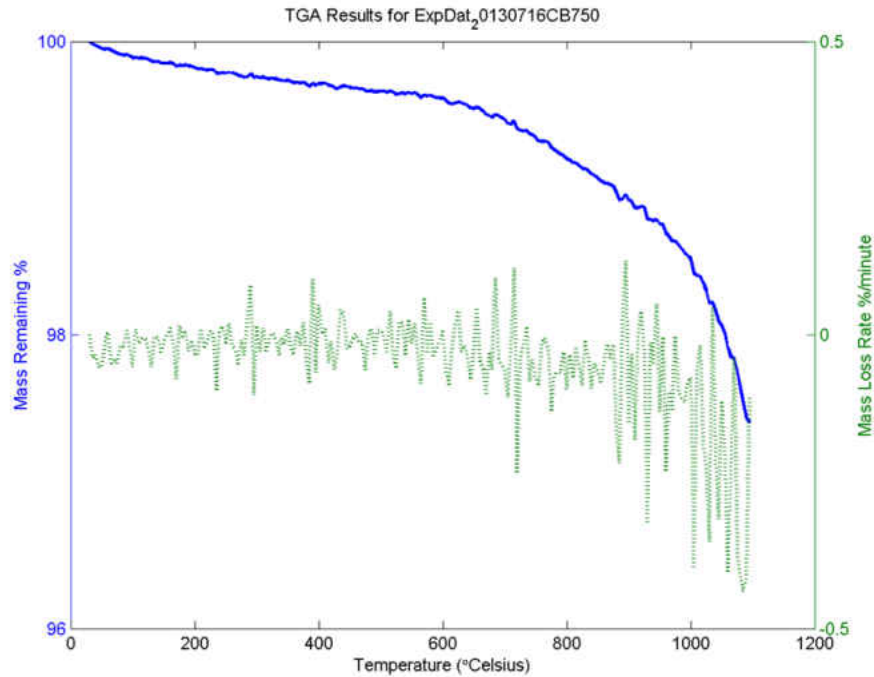
Figure 13: TGA of basalt-carbon composite

4.2   Effect of Pyrolysis on Fiber-Reinforced Composite Properties

4.2.1 Pyrolysis Mass Effect

As expected, the pyrolysis of PMCs converts the polymeric matrix into carbon, and in doing so reduces the total mass of the FRC. Table 1 shows the percentage of mass loss for the two types of fiber reinforcement used with the phenolic resin matrix from the pyrolysis process. Interestingly, the mass loss percentage of the basalt FRC loses 4% less mass than the carbon FRC. This suggests that a larger amount of carbon is being retained in the basalt FRC than the carbon FRC, either from literal retention or from the aforementioned induced carbon growth. It is safe to assume from the previously discussed analysis of basalt-carbon morphology that the mechanism of carbon growth due to the

29

composition of basalt is the likely culprit. Also, the shrinkage of the basalt FRC and densification of the matrix (and reduction of porosity) in particular could promote a higher level of hydrocarbon retention during the conversion process, leading to a larger amount of carbonaceous residue remaining in the finished product.

Table 1: Average Pyrolysis Mass Loss Percentage

Matrix Conversion	*%*
Carbon Phenolic to Carbon-Carbon	-18.6%
Basalt-Phenolic to Basalt-Carbon	-14.8%

4.2.2 Thermal Effect

ASTM-E285 specifies a series of calculations to be made to parameterize the effectiveness of thermal materials in a comparable fashion. Three categories are sufficient for thermal screening: temperature gradient, insulation index, and erosion rate. Four types of materials are tested to establish a baseline and to make comparisons after applying the designed pyrolysis cycle: carbon-phenolic, carbon-carbon, basalt-phenolic, and basalt-carbon. The time-temperature plots portrayed in the upcoming section is normalized to ambient temperature for easier comparison, with the time period beginning at initial flame impingement and ending at material burn-through.

Figure 14 displays the time-temperature plot for Carbon-Phenolic. Several notable features arise in the tracking of the temperature gradient. Back-side temperature of all three panels tested adhere to ambient conditions for approximately 12 seconds before an exponential rise. A steady increase is visible until approximately 250°C where a small plateau occurs. No observed physical changes occurred during testing at this juncture, suggesting that this event is material composition based.

Figure 14: Normalized time-temperature curve for Carbon-Phenolic

Figure 15 displays the time-temperature plot for Carbon-Carbon. Several notable features arise in the tracking of the temperature gradient. Back-side temperature of all three panels tested adhere to ambient conditions for approximately 6 seconds before an exponential rise. A steady increase is visible until approximately 100°C where an extended plateau of approximately 7 seconds occurs. No observed physical changes occurred during testing at this juncture, suggesting that this event is material composition based. This plateau is followed by a distinctive small plateau at 250°C also witnessed in Carbon-Phenolic. Again, no observed physical changes occurred during testing at this juncture.

Figure 15: Normalized time-temperature curve for Carbon-Carbon

Figure 16 displays the time-temperature plot for Basalt-Phenolic. Several notable features arise in the tracking of the temperature gradient. Back-side temperature of all three panels tested adhere to ambient conditions for approximately 7 seconds before an exponential rise. A steady increase is visible until approximately 250°C where a small plateau occurs, as observed in the previous carbon FRC panels. No observed physical changes occurred during testing at this juncture, suggesting that this event is material composition based.
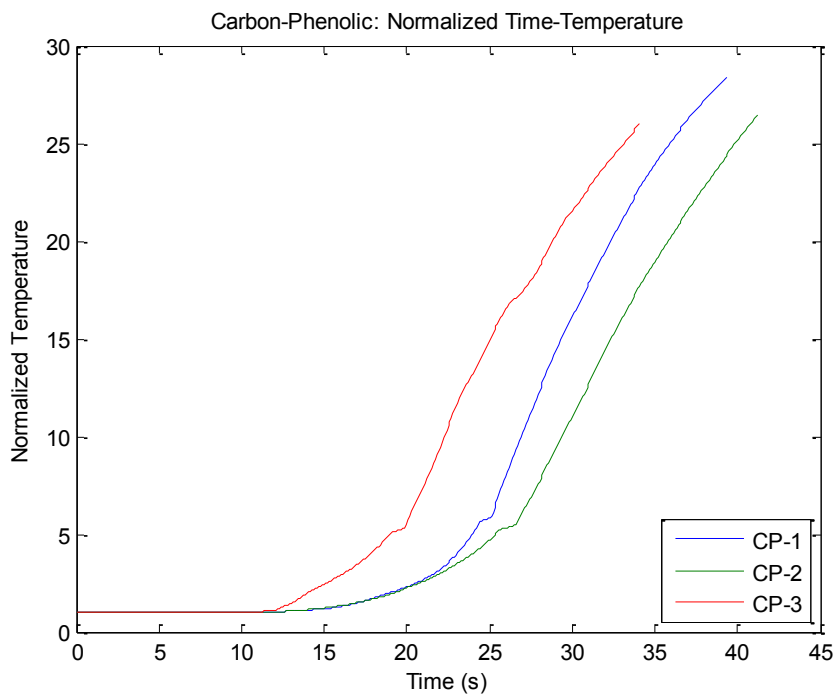

Figure 16: Normalized time-temperature curve for Basalt-Phenolic

Figure 17 displays the time-temperature plot for Basalt-Carbon. Several notable features arise in the tracking of the temperature gradient. Back-side temperature of all three panels tested adhere to ambient conditions for approximately 5 seconds before an exponential rise. A steady increase is visible until approximately 100°C where an extended plateau of approximately 7 seconds occurs, reminiscent of the plateau in carbon-carbon. No observed physical changes occurred during testing at this juncture, suggesting that this event is material composition based. This plateau is followed by a distinctive small plateau at 250°C also witnessed in all test samples. Again, no observed physical changes occurred during testing at this juncture.
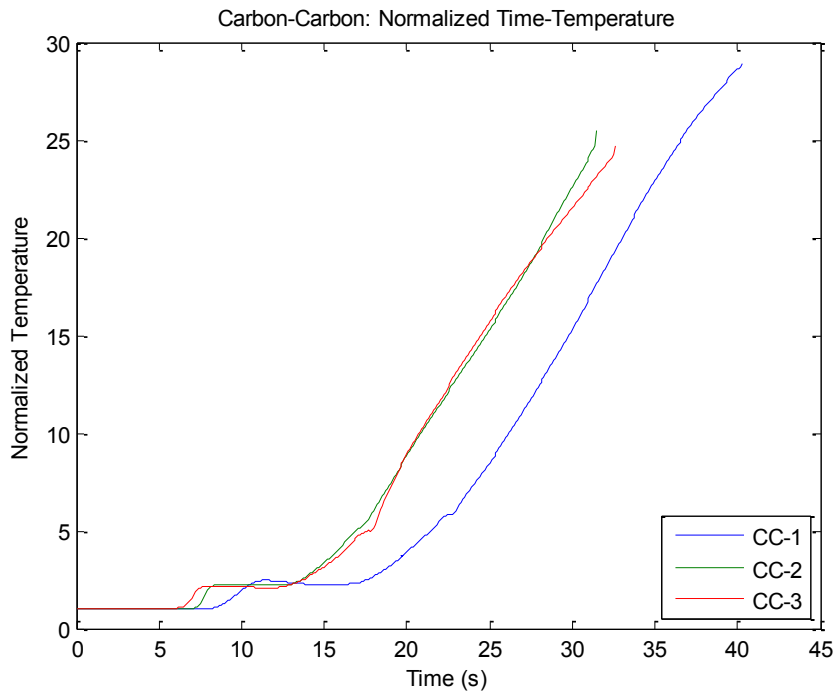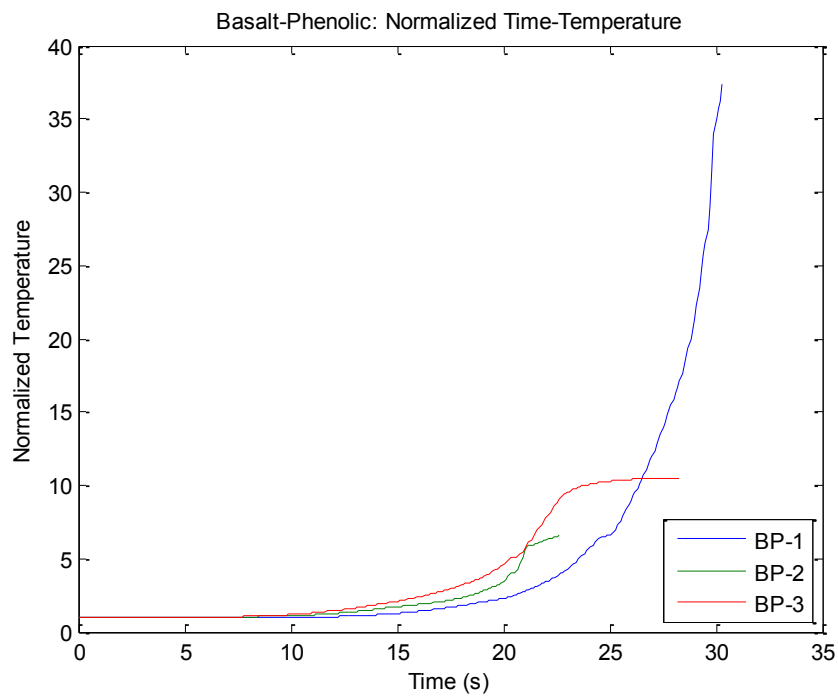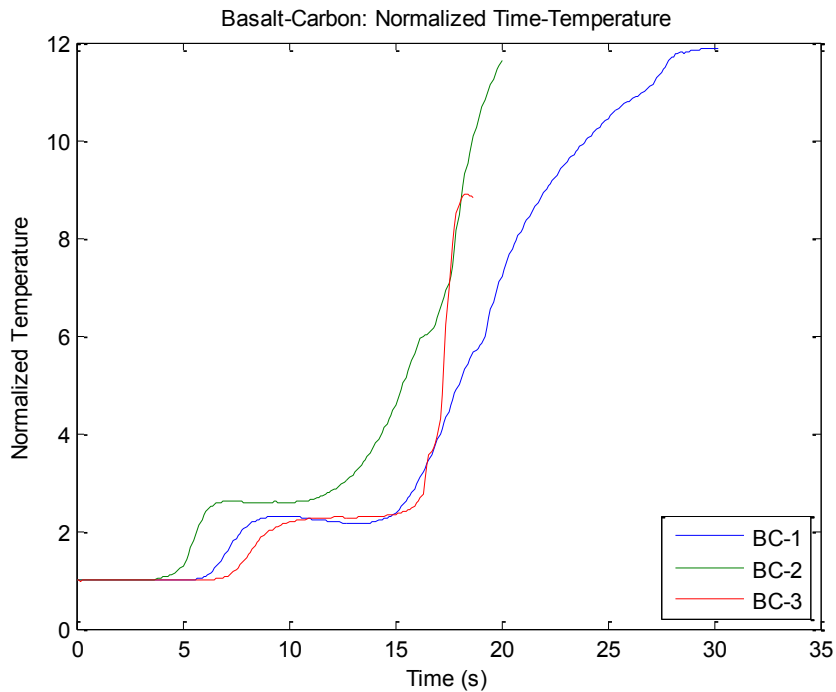

Figure 17: Normalized time-temperature curve for Basalt-Carbon

Several distinct trends arise from the oxyacetylene testing of the four sample types. These features are undoubtedly attributable to the material composition, fiber and matrix. Before any juxtapositions are made, it is of note that no physical and/or mechanical failure was observed in any of the test samples, regardless of composition. This criteria of failure encompasses: delamination of any sort in any direction, cracking, fracture, or loss of integrity during thermal testing.

Firstly, all four material types display a small plateau near 250°C, implying a thermomechanical phenomenon associated with carbonaceous residue at this temperature.

Secondly, phenolic-matrix FRCs adhere to ambient temperatures for a longer period. This observation is immediately related to the existence of a polymeric structure undergoing ablation. The ablation of the matrix releases gases from chemical and phase changes that introduce convective heat transfer in addition to pure conduction. This convective process is lacking in pure carbon-matrix composites.

Thirdly, carbon-matrix FRCs demonstrate an extended low temperature plateau at 100°C. An unmistakable correlation to the matrix is clearly evidenced. This low temperature phenomenon is attributable to the homogenization of the material properties, both in-plane and interlaminar. A unique distinction arises with the matching of thermal properties, as stimulating more isotropic properties mitigates thermal shock and consequently, lessens the chance of delamination or failures from large thermal gradients.

<u>4.2.2.2   Insulation</u>

ASTM-E285 defines insulation index as a material parameter measuring the insulating effectiveness of the material. This value is taken at three milestones, as shown in Table 2. It is a ratio of the time to reach temperature to the thickness of the material. The higher the value, the better insulator the material is under the applied test conditions. Three observable trends can be discerned from the data presented in Table 2.

Firstly, carbon FRCs perform significantly better than their basalt FRC counterpart. An immediate realization is that the working temperature of the fiber reinforcement. Under the extreme conditions of the oxyacetylene flame, the basalt fiber begins to erode and melt away at a much earlier time than carbon fiber. Post testing observation shows a conspicuous burning pattern and burn-through hole in the basalt FRC samples. Additionally there is a glassy residue, including beading, highly evident on the front surface of the basalt samples, whereas the carbon FRCs show little to no physical changes.

Secondly, carbon-matrix FRC's underperform in comparison to their phenolic-matrix counterparts. Again, this is due to the existence of convective heat transfer caused by the ablation of the polymeric matrix.

Thirdly, the decrease in insulation index for the same fiber but different matrix is almost identical. This is a measurable development that can be correlated to the mechanisms surrounding the ablation of the polymeric matrix.

Table 2: Average Insulation Index (s/m)

Material	*80°C*	*180°C*	*380°C*
Carbon-Phenolic	3118 s/m	3654 s/m	4142 s/m
Carbon-Carbon	2483 s/m	2976 s/m	3549 s/m
Basalt-Phenolic	3087 s/m	3475 s/m	3984 s/m
Basalt-Carbon	2388 s/m	2730 s/m	3528 s/m

4.2.2.3   Erosion

ASTM-E285 defines erosion as a material parameter in the form of erosion rate. This value measures survivability of the material as a ratio of the thickness to the time to burn-through. The smaller the value, the better erosion resistance the material possesses under the applied test conditions. Two observable trends can be discerned from the data presented in Table 3.

Firstly, carbon reinforcement is clearly better than basalt reinforcement under the applied test conditions. Not only is the erosion rate significantly lower, the burn-through times are noticeably longer as well. This was a predictable result purely associated with the working temperature of the reinforcement material. It is of note that the matrix conversion reduced the erosion resistance of carbon FRC much less than basalt FRC. This is due to a physical detachment of the matrix from mechanical loads applied to the test samples. As shown previously, the basalt-carbon-matrix is a much denser material with better interfacial bonding of the fiber and matrix, thus the damaging of the material is more consistent with the removal of carbon and fiber simultaneously. However the reduction in

burn-through time is very close for both reinforcements, suggesting that the matrix composition, both chemically and physically, have a large influence on erosion resistance.

Table 3: Average Erosion Rate (m/s) and Burn-Through Time (s)

Material	*Erosion Rate*	*Burn-Through Time*
Carbon-Phenolic	0.000167 m/s	38.2 s
Carbon-Carbon	0.000185 m/s	34.8 s
Basalt-Phenolic	0.000238 m/s	27.1 s
Basalt-Carbon	0.000289 m/s	23.0 s

While the erosion rate is highly indicative of the physical changes induced in the panel from high-temperature exposure, the mass loss is more telling of the microscale morphological and composition changes occurring in the materials. Table 4 shows a high discrepancy between the mass loss experienced by the two types of reinforcing fibers. While carbon fiber again shows a small change when converting the matrix material in comparison to the change in basalt fiber, the magnitude of the mass loss percentage is much more favorable to basalt reinforcement. Echoing the results from TGA of basalt-carbon, the mass loss is minuscule when physical changes are considered. Since the basalt fiber shows substantial physical damage, including loss of material, in comparison to the minimal damage sustained by the carbon fiber, basalt-carbon appears to dissipate heat better than carbon as it is abler in sustaining the matrix and interface under loading.

Table 4: Average Post-ASTM-E285 Mass Loss Percentage

Material	*%*
Carbon-Phenolic	-10.9%
Carbon-Carbon	-9.9%
Basalt-Phenolic	-8.4%
Basalt-Carbon	-5.4%

4.2.3   Mechanical Effect

4.2.3.1   Bending Strength

ASTM-D790 specifies a series of calculations to parameterize the flexural properties of reinforced materials from bending stresses. Three-point bending is used to establish modulus for the four types of materials tested: carbon-phenolic, carbon-carbon, basalt-phenolic, and basalt-carbon. Figure 18 presents a portion of the linear displacement-strain curve for all four materials.

It is immediately noticeable that carbon-carbon and basalt-carbon overlap, suggesting that the pyrolysis process effectively changed the mechanical failure mechanism from fiber-dominated to matrix-dominated as expected. A more telling trend is how similar the measured values are. Recall that this test is not representative of the tensile behavior of the materials, but of the ply-stacking sequence; this is indicative of consistency in manufacturing and processing of the four materials and the similarities in the moduli of the fiber reinforcements..
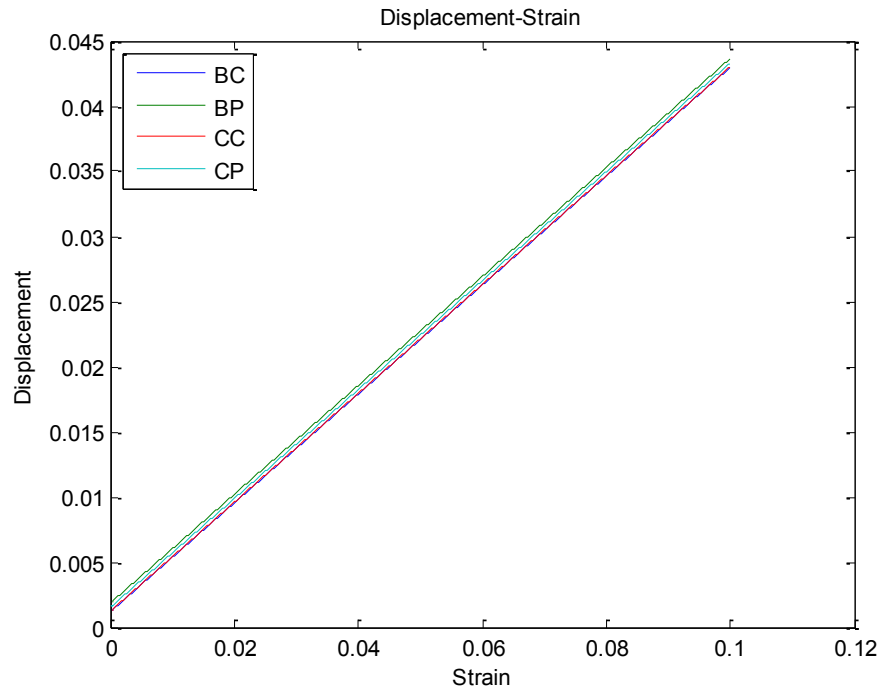
Figure 18: Three-Point Bending Displacement-Strain

While mildly indistinguishable, the pyrolysis process had an adverse effect on carbon reinforcement, whereas the pyrolysis process positively affected the basalt reinforcement. Table 5 shows the maximum stress experienced by the outer fiber of the sample and the calculated modulus from the linear portion of the flexural data. Interestingly, the reduction of carbon FRC modulus from pyrolysis is contradictory to the increase of basalt FRC modulus. This can be explained by both physical and morphological changes in the materials when pyrolyzed.

As the carbon FRC is pyrolyzed, the conversion of the phenolic into carbon is processed in the same manner as the basalt FRC. However, an obvious volumetric shrinkage occurs during the low-temperature treatment of the basalt FRC. This shrinkage

has a densifying effect on the basalt FRCs that is not experienced by carbon FRCs. By extension, the void content of the carbon-carbon is much higher than that of the basalt-carbon. Compounded with the verified growth of mechanically-attached organized carbon on the basalt fiber, the defects exhibited by the laminates is increased in carbon FRC pyrolysis and decreased in basalt FRC. Additionally, the objective of homogenizing fiber and matrix properties was realized more effectively in the basalt fiber than the carbon fiber.

Table 5: Average Maximum Bending Stress (MPa) and Modulus (GPa)

	Maximum Stress	_Modulus_
Carbon-Phenolic	44.85 MPa	34.24 GPa
Carbon-Carbon	38.62 MPa	29.53 GPa
Basalt-Phenolic	35.57 MPa	27.00 GPa
Basalt-Carbon	37.27 MPa	28.41 GPa

CHAPTER FIVE: CONCLUSIONS

Pyrolysis of a polymer-matrix into a carbon-matrix composite drastically affects both thermal and mechanical properties of FRCs. While this concept is not a new technology, the approach used in this research presents a novel implementation of conventional materials in a low-cost, in-situ manufacturing and processing cycle. The evidence of carbon growth on basalt fiber without the use of catalytic precursors poses possibly innovative solutions to designing more effective high-temperature composites.

Table 6 shows a summary of the property changes measured and/or calculated through this research. While basalt reinforced composites performed poorly under the applied thermal conditions, they excelled mechanically. Despite the thermal shortcomings demonstrated by basalt fibers, several positive conclusions can be made about the usefulness of this new basalt-carbon material.

Table 6: Average Pyrolysis Property Change Percentage

	CP to CC	BP to BC
% Insulation Index @ 80°C	-20.4	-22.6
% Insulation Index @ 180°C	-18.6	-21.4
% Insulation Index @ 380°C	-14.0	-11.5
% Burn-Through Time	-9.0	-15.1
% Erosion Rate	+10.3%	+21.3%
% Average Maximum Stress	-13.9	+4.8
% Average Modulus	-13.7	+5.3

The thermal applicability of basalt-carbon is clearly not applicable to the type of thermal exposure used in this research. However, TGA initially indicated a thermal stability of basalt-carbon up to and beyond 600°C. This was further evidenced by the plateau in the ASTM-E285 mass loss calculations. ASTM-E285 is normally used as an ablative screening test, which operates well outside of the working range of basalt fibers. It is highly possible that this material is useful as a lower temperature insulator and structural material. Furthermore, the objectives set out in this research were met by the unique processing techniques that yielded the basalt-carbon material; the FRC was successfully densified as proven by SEM imaging; the polymer matrix was converted to carbon and shown in SEM, RS, and EDX; the fiber-matrix interface was improved via the mechanical attachment of carbon growth on the basalt fiber, shown by SEM; and the homogenization of fiber and matrix properties was achieved, proven thermally from temperature gradient and mechanically from three-point bending.

Additional testing is necessary to fully evaluate the practicality of basalt-carbon. Thermally, the poor performance should be relieved by reducing the thermomechanical loading, either by changing any of temperature, pressure/force, and area versus point impingement. Steady-state insulation and/or conductivity tests should be performed to completely characterize the thermal effectiveness of the material. Mechanically, a mixed mode test will further measure the interfacial improvements brought about by pyrolysis. The inclusion of shear stresses on composites is a strong method of failure, and an important area in FRC research. Impact testing is also prudent as the change in mechanical failure from fiber-dominated to matrix-dominated leads to brittle fracture.

Notwithstanding, much work is left to be done that is outside of the scope of this research. Primarily, the carbon conversion/growth mechanism must be optimized. A supply limitation rather than a diffusion limitation potentially allows carbon structures to form more slowly at the catalytic sites, encouraging carbon structures to anneal to the lowest level configuration. [12] This issue may have prevented better organization and quality of carbon to be produced, as a possible overabundance of hydrocarbon precursor potentially stunts growth. Furthermore, the formation of pyrolytic carbon structures varies on the mechanism that the carbon deposits from the gas phase. This is affected by gas particle size as well as gas circulation. [33] The size of gaseous hydrocarbon particles can be inhibit the level of penetration through the laminate as the density rapidly increases while porosity decreases. This may also stunt the growth and quality of the resulting carbon or induce different densities, porosities, carbon content, and properties in the laminate.

Further investigations of the existing processes include designing for specific thermomechanical loadings. This entails the use of different stacking sequences and possible material hybridization (polymer reinfiltration, additional treatments, mixing of fiber reinforcements, etc.). When considering specific operating temperatures, an inquiry into both the 100°C and 250°C phenomena could reap massive rewards, including a better understanding of thermal fatigue. All of these options require a deeper understanding of qualitative and quantitative mechanisms that lead to thermomechanical failure and high-temperature degradation of carbon-matrix composites, and basalt-carbon in particular.

APPENDIX A: CARBON FIBER DATA

Tensile Fiber Properties	US Units	SI Units
Tensile Strength		
6K	800ksi	5515 MPa
12K	820 ksi	5655 MPa
Tensile Modulus (Chord 6000-1000)	40.0 Msi	276 GPa
Ultimate Elongation at Failure		
6K	1.9%	1.9%
12K	1.9%	1.9%
Density	0.0643 lbm/in^3	1.78 g/cm^3
Weight/Length		
6K	12.5 x 10^{-6} lb/in	0.223 g/m
12K	25.0 x 10^{-6} lb/in	0.446 g/m
Approximate Yield		
6K	6674 ft/lb	4.48 m/g
12K	3337 ft/lb	2.24 m/g
Tow Cross-Sectional Area		
6K	1.94 x 10^{-4} in^2	0.13 mm^2
12K	3.89 x 10^{-4} in^2	0.25 mm^2
Filament Diameter	0.203 mil	5.2 microns
Carbon Content	95.0%	95.0%
Twist	Never Twisted	Never Twisted

APPENDIX B: BASALT FIBER DATA

Thermal	Working temperature	-452 – 1292 ºF
	Felting temperature	1922 ºF
	Thermal coefficient	0.03 – 0.038 W/m·ºK
Physical	Diameter of filament	7 – 15 μm
	Density	165 lbm/ft^3
	Elastic modular	100—110 GPa
	Tensile strength	600 – 696 ksi
	Tensile strength @	
	68 ºF	100%
	392 ºF	95%
	752 ºF	82%
Chemical	Weight loss after 3hr boiling	
	2M HC1	2.2%
	2M NaOH	6%
	H_2O	0.2%

| Type of fiber	Density (lbm/ft^3)	Tensile (ksi)	Elastic modulus (GPa)	Elongation (%)
Glass fiber				
A style	153	480	69	4.8
C style	153	480	69	4.8
E style	162	500	76	4.76
S-2 style	155	700	97	5.15
Silica fiber	135	30 – 60		
Quartz fiber	137	499		
Carton fiber				
large tow	108	525	228	1.59
medium tow	112	740	241	2.11
small tow	112	900	297	2.2
Aromatic Polyamide fiber				
Kevlar 29	90	525	41	3.6
Kevlar 149	92	505	186	1.5
Polypropylene fiber	57	39 – 94	38	15 – 18
Polyolefin fiber	74	72 – 132	75	11 – 20
Basalt fiber	165	600 -- 696	100 -- 110	3.3

APPENDIX C: IMAGES OF POST-ASTM-E285 SAMPLES
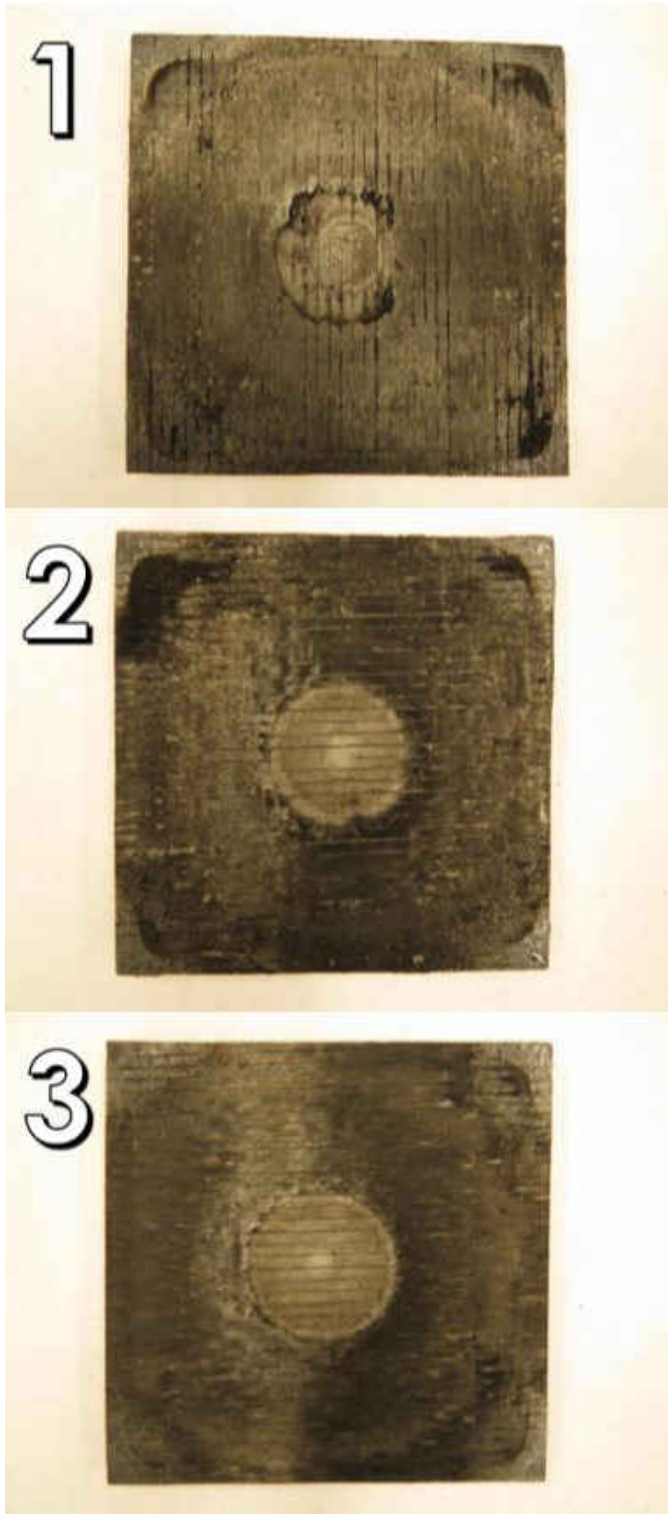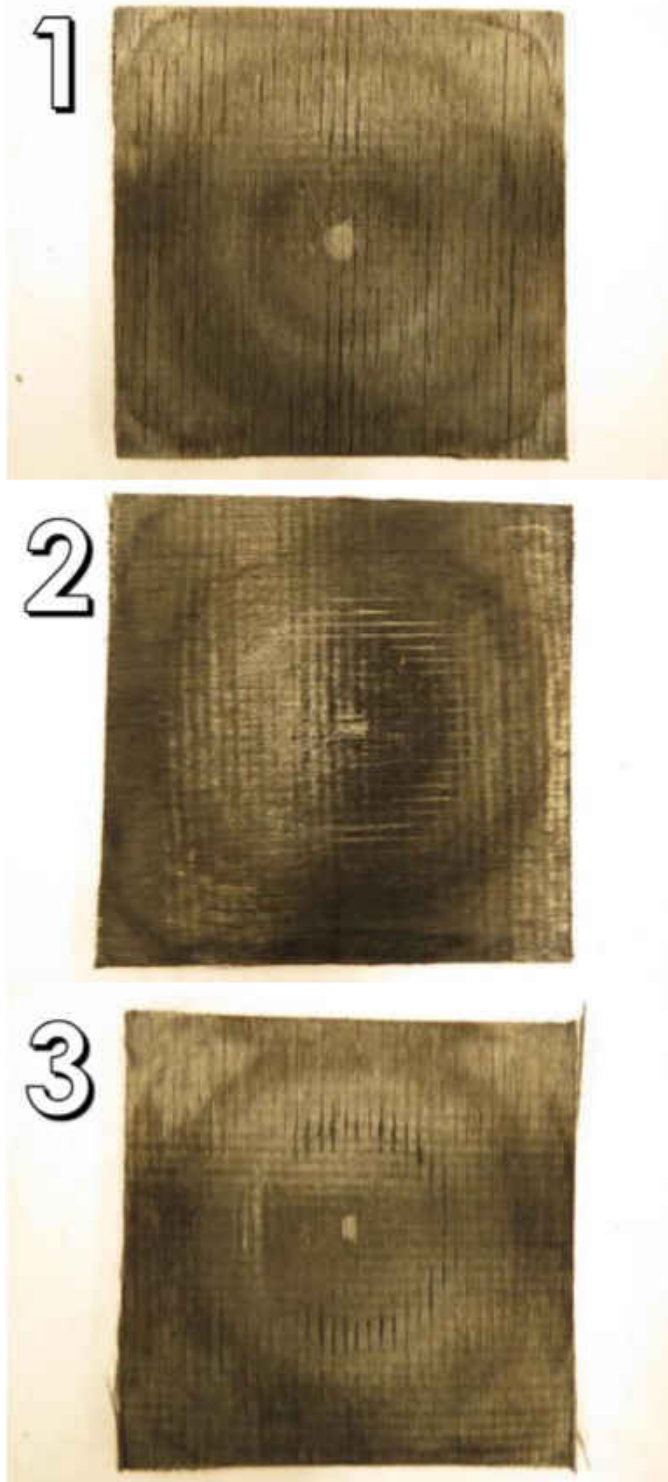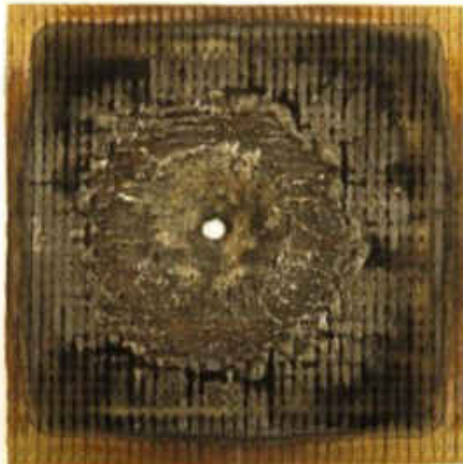
Figure 19: Carbon-Phenolic Post-ASTM-E285
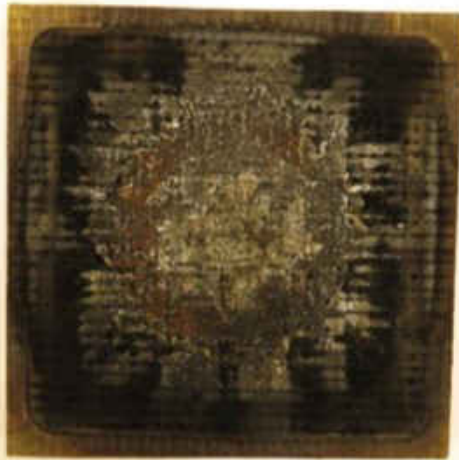
Figure 20: Carbon-Carbon Post-ASTM-E285

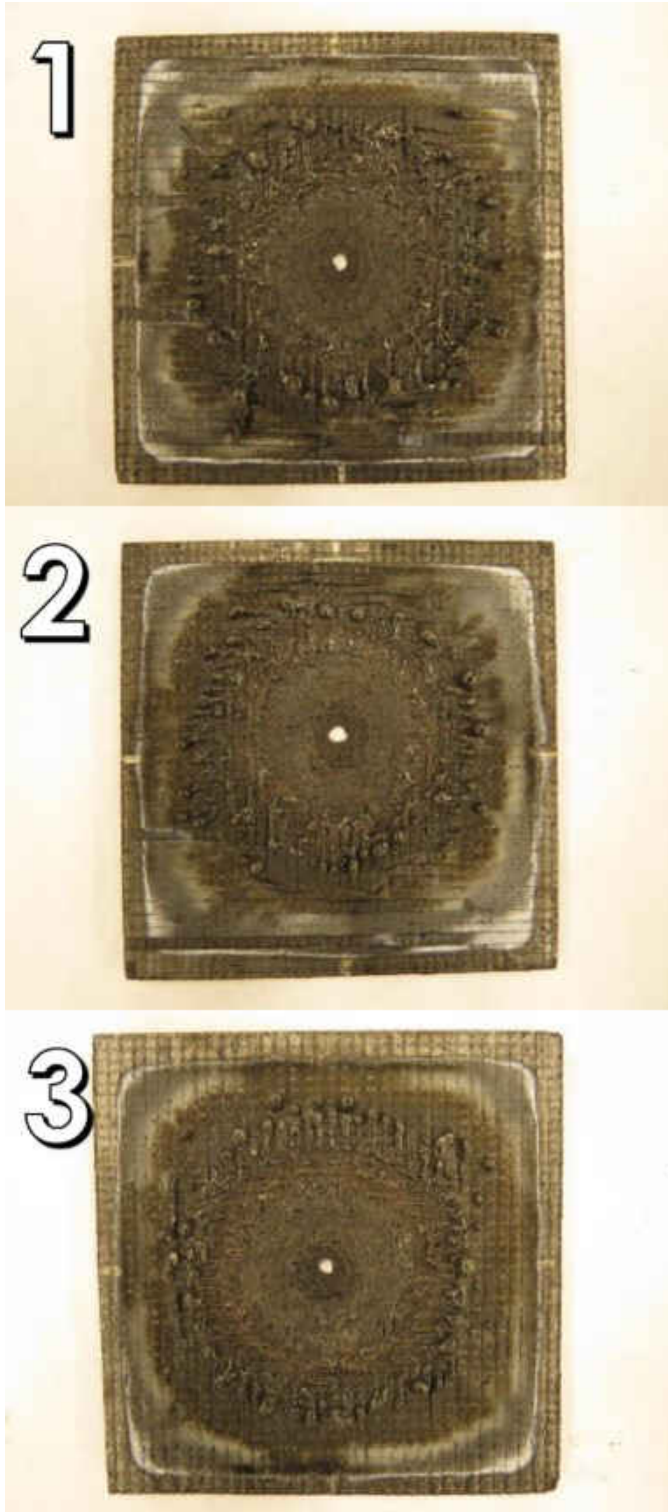Figure 21: Basalt-Phenolic Post-ASTM-E285

Figure 22: Basalt-Carbon Post-ASTM-E285

REFERENCES

1. Bahramian, A. R., et al. (2006). "Ablation and thermal degradation behaviour of a composite based on resol type phenolic resin: Process modeling and experimental." Polymer **47**(10): 3661-3673.

2. Patton, R. D., et al. (2002). "Ablation, mechanical and thermal conductivity properties of vapor grown carbon fiber/phenolic matrix composites." Composites Part A: Applied Science and Manufacturing **33**(2): 243-251.

3. Park, J. K., et al. (2004). "A comparison of the interfacial, thermal, and ablative properties between spun and filament yarn type carbon fabric/phenolic composites." Carbon **42**(4): 795-804.

4. Kang, T. J., et al. (2006). "Mechanical, thermal and ablative properties of interply continuous/spun hybrid carbon composites." Carbon **44**(5): 833-839.

5. Cho, D. and B. Il Yoon (2001). "Microstructural interpretation of the effect of various matrices on the ablation properties of carbon-fiber-reinforced composites." Composites Science and Technology **61**(2): 271-280.

6. Park, J. K. and T. J. Kang (2002). "Thermal and ablative properties of low temperature carbon fiber–phenol formaldehyde resin composites." Carbon **40**(12): 2125-2134.

7. Chen, W., et al. (2009). "Basalt fiber–epoxy laminates with functionalized multi-walled carbon nanotubes." Composites Part A: Applied Science and Manufacturing **40**(8): 1082-1089.

8. Černý, M., et al. (2009). "Partially pyrolyzed composites with basalt fibres – Mechanical properties at laboratory and elevated temperatures." Composites Part A: Applied Science and Manufacturing **40**(10): 1650-1659.

9. Colombo, C., et al. (2012). "Static and fatigue characterisation of new basalt fibre reinforced composites." Composite Structures **94**(3): 1165-1174.

10. Lee, J. H., et al. (2010). "The tensile and thermal properties of modified CNT-reinforced basalt/epoxy composites." Materials Science and Engineering: A **527**(26): 6838-6843.

11. Norinaga, K., et al. (2006). "Analysis of gas phase compounds in chemical vapor deposition of carbon from light hydrocarbons." Carbon **44**(9): 1790-1800.

12. Hafner, J. H., et al. (1998). "Catalytic growth of single-wall carbon nanotubes from metal particles." Chemical Physics Letters **296**(1–2): 195-202.

13. Li, Q., et al. (2004). "Effect of hydrocarbons precursors on the formation of carbon nanotubes in chemical vapor deposition." Carbon **42**(4): 829-835.

14. Hernadi, K., et al. (1996). "Fe-catalyzed carbon nanotube formation." Carbon **34**(10): 1249-1257.

15. Norinaga, K. and K. J. Hüttinger (2003). "Kinetics of surface reactions in carbon deposition from light hydrocarbons." Carbon **41**(8): 1509-1514

16. Colomer, J. F., et al. (2000). "Large-scale synthesis of single-wall carbon nanotubes by catalytic chemical vapor deposition (CCVD) method." Chemical Physics Letters **317**(1–2): 83-89.

17. Sinnott, S. B., et al. (1999). "Model of carbon nanotube growth through chemical vapor deposition." Chemical Physics Letters **315**(1–2): 25-30.

18. Hernadi, K., et al. (2000). "Production of nanotubes by the catalytic decomposition of different carbon-containing compounds." Applied Catalysis A: General **199**(2): 245-255.

19. Dong, G. L. and K. J. Hüttinger (2002). "Consideration of reaction mechanisms leading to pyrolytic carbon of different textures." Carbon **40**(14): 2515-2528.

20. Belin, T. and F. Epron (2005). "Characterization methods of carbon nanotubes: a review." Materials Science and Engineering: B **119**(2): 105-118.

21. Colomer, J. F., et al. (2001). "Characterization of single-wall carbon nanotubes produced by CCVD method." Chemical Physics Letters **345**(1–2): 11-17.

22. Gong, Q.-m., et al. (2005). "The effect of carbon nanotubes on the microstructure and morphology of pyrolytic carbon matrices of C–C composites obtained by CVI." Composites Science and Technology **65**(7–8): 1112-1119.

23. Taylor, C. A., et al. (2004). "Microstructural characterization of thin carbon films deposited from hydrocarbon mixtures." Surface and Coatings Technology **182**(2–3): 131-137.

24. Chatzigeorgiou, G., et al. (2012). "Effective mechanical properties of "fuzzy fiber" composites." Composites Part B: Engineering **43**(6): 2577-2593.

25. Yamamoto, N., et al. (2012). "Electrical and thermal property enhancement of fiber-reinforced polymer laminate composites through controlled implementation of multi-walled carbon nanotubes." Composites Science and Technology **72**(16): 2009-2015.

26. Bafekrpour, E., et al. (2013). "A novel carbon nanofibre/phenolic nanocomposite coated polymer system for tailoring thermal behaviour." Composites Part A: Applied Science and Manufacturing **46**(0): 80-88.

27. Bafekrpour, E., et al. (2013). "Preparation and properties of composition-controlled carbon nanofiber/phenolic nanocomposites." Composites Part B: Engineering **52**(0): 120-126.

28. Shi, R., et al. (1997). "Deposition mechanism of pyrolytic carbons at temperature between 800–1200 °C." Carbon **35**(12): 1789-1792.

29. Liang, F., et al. (2012). "Effect of the addition of carbon black and carbon nanotubes on the structure and oxidation resistance of pyrolysed phenolic carbons." New Carbon Materials **27**(4): 283-287.

30. Tzeng, S.-S. and Y.-G. Chr (2002). "Evolution of microstructure and properties of phenolic resin-based carbon/carbon composites during pyrolysis." Materials Chemistry and Physics **73**(2–3): 162-169.

31. Trick, K. A., et al. (1997). "A kinetic model of the pyrolysis of phenolic resin in a carbon/phenolic composite." Carbon **35**(3).

32. Trick, K. A. and T. E. Saliba (1995). "Mechanisms of the pyrolysis of phenolic resin in a carbon/phenolic composite." Carbon **33**(11): 1509-1515.

33. Je, J. H. and J. Y. Lee (1984). "A study on the deposition of pyrolytic carbons from hydrocarbons." Carbon **22**(6): 563-570.

34. Pilato, L. (2013). "Phenolic resins: 100 Years and still going strong." Reactive and Functional Polymers **73**(2): 270-277.